Fluid Phase Equilibria 462 (2018) 85–99

Contents lists available at ScienceDirect

Fluid Phase Equilibria

journal homepage: www.elsevier.com/locate/fluid

Study on thermo physical properties of binary mixture containing aromatic alcohol with aromatic, substituted aromatic amines at different temperatures interms of FT-IR, ^{1}H NMR spectroscopic and DFT method

M. Raveendra [a], M. Chandrasekhar [b], K. Chandrasekhar Reddy [c], A. Venkatesulu [d], K. Sivakumar [e, *], K. Dayananda Reddy [a, **]

[a] Department of Chemistry, P.V.K.N. Govt. Degree & P.G. College, Chittoor, 517001, A.P., India
[b] Department of Physics, Wollega University, Nekemte, Ethiopia
[c] Department of Physics, SSBN Degree College, Anantapur, A.P., India
[d] Department of Physics, Govt. First Grade College, Hosakote, Bangalore Rural, Karnataka, 583101, India
[e] Department of Chemistry, S.V. Arts Degree & P.G.College (T.T.D'S), Tirupati, 517502, A.P., India

ARTICLE INFO

Article history:
Received 13 October 2017
Received in revised form
14 January 2018
Accepted 22 January 2018

Keywords:
Intermolecular interaction
Binary mixture
Excess property
DFT
MD
NMR
FT-IR

ABSTRACT

The densities (ρ) of binary mixtures of benzyl alcohol (BA) with aniline (A), N-methylaniline (NMA), *N,N*-dimethylaniline (NNDMA), *o*-chloroaniline (*o*-CA) and *m*-chloroaniline (*m*-CA) have been analysis at different temperatures. Further, the speeds of sound (u) were measured at 303.15 K and 313.15 K temperatures of the above said systems. The excess molar volumes (V^E) and excess isentropic compressibilities (κ_S^E) calculated by using experimental data. The measured thermo physical properties were fitted in terms of R.K & HW equations. The measured u values were compared with Jacobson's free length theory (FLT) and Schaff's collision factor theory (CFT). The experimental and theoretical investigations have been playing a dominant role in the elucidation of hydrogen bond in solute, solvent and solute-solvent of the mixture. The results has been further confirmed by the existence of solvent-solute interactions of hydrogen bonding between benzyl alcohol and amines through Fourier transform Infrared and Nuclear Magnetic Resonance data at equimolar composition. The analysis of intermolecular hydrogen bond association through electron density, natural bond orbital analysis using density functional theory (DFT). The position and design of intensity of −OH and $-NH_2$ bands as per Nuclear Magnetic Resonance and Fourier transform Infrared spectroscopic data strongly supported by the conclusion that molecular association of inter molecular hydrogen bonding through excess properties have been observed. Further, the molecular dynamics (MD) simulations have been performed in liquid phase used to calculate the radial distribution functions of the pure components and mixtures with equimolar mole fractions at 298.15 K and 1 atm. From the molecular dynamics simulation and quantum calculations it has been confirmed the existence of H-bond between component molecules.

1. Introduction

Thermo physical properties of binary liquid mixtures, having molecules that measure ready for undergoing interactions, show vital deviation from ideality due to arising of structural changes. Systematic experimental study on thermo physical properties of binary mixtures is being an important tool/guide for the investigation of the molecular interactions. The derivation of various excess functions from the measured properties of individual pure and of mixture components and the analysis of the latter in terms of applications of several statistical theories of solutions give a better understanding of interactions present at molecular level. Moreover, the present experimental work on density (ρ) and speed of sound

* Corresponding author. Tel.: +91 9290080843.
** Corresponding author. Tel.: +919440359792.
E-mail addresses: sivakumarkasi64@gmail.com (K. Sivakumar), dayakollu@gmail.com (K. Dayananda Reddy).

https://doi.org/10.1016/j.fluid.2018.01.025
0378-3812/

(u) of binary systems are important not only to sensible viewpoint, but also towards theoretical consideration. The investigation of the speed of sound is one of the valuable relatively simple and reliable tool for the study of liquids and liquid mixtures. Further, the chemical industries have identified the key role of the thermodynamic properties involving in design calculations for chemical separation, heat and mass transfer and fluid flow. When two or more component molecules are mixed with one another to form a liquid mixture, it causes a drastic effect on the properties of resulting solution and differences in the intermolecular interactions of component molecules.

The solvent-solute interactions between liquid molecules interms of excess thermodynamic functions produce a vital role within the development of molecular sciences and structural arrangement of the molecules [1,2]. Generally, present studying systems play a key role in different biological applications such as protein folding [3,4], membrane assembly [5], electrochemical cells [6] and heterogeneous catalysis [7]. The liquids that were selected within the investigation having a variety of commercial applications. Benzyl alcohol is utilized as versatile solvent in the synthesis of perfuming products and in veterinary medicines [8]. The utility of amines involves in pharmaceutical, agricultural, rubber chemicals. The industrial importance of chloroaniline is vast which include in oil solvents, fungicides and an intervening agent in the synthesis of azo dyes, agricultural chemicals and prescription drugs. Aniline is the starting material in the dye manufacturing industry. It forms aniline colors when combined with other substances, particularly chlorine or chlorates. Aniline is also important in the manufacture of rubber-processing chemicals, explosives, plastics, antioxidants and varnishes. Amines take part in many kinds of chemical reactions and offer many industrial applications. *o*-chloroaniline is used as an intermediate in the production of a number of products, including agricultural chemicals, azo dyes and pigments and pharmaceuticals. *o*-chloroaniline is also used in petroleum solvents and fungicides. dimethylaniline is a key precursor to commercially important triarylmethane dyes such as malachite green and crystal violet. Dimethylaniline serves as a promoter in the curing of polyester and vinyl ester resins. Dimethylaniline is also used as a precursor to other organic compounds. A study of the in vitro metabolism of *N,N*-dimethyl aniline using guinea pig and rabbit preparations and GLC techniques has confirmed *N*-demethylation and *N*-oxidation as metabolic pathways, and has also established ring hydroxylation as a metabolic route [9]. The study of excess thermodynamic properties like V^E and κ_S^E of binary mixtures of benzyl alcohol and amines interms of spectral data are much of great significance to know the molecular interactions in binary liquid components in order to experience and to analysis the applicability of various solution theories and mathematical models [10].

In this research work, new experimental data report on density (ρ) and speed of sound (u) for the binary mixtures of benzyl alcohol with aniline (A), N-methylaniline (NMA), *N,N*-dimethylaniline (NNDMA), *o*-chloroaniline (*o*-CA) and *m*-chloroaniline (*m*-CA). Moreover, the experimental data were further confirmed by elucidation of hydrogen bonding between benzyl alcohol molecule and amine. The −OH group of benzyl alcohol also can act as proton acceptor due to lone electron pairs on oxygen atom and anilines which contain $-NH_2$ group serves as a π-type donor.

The measured u data for the studying systems were contrast in terms of CFT [11] and FLT [12,13] to check capability of these theories. FT-IR and NMR spectroscopic analysis were additionally collected within the present investigation to understand the prevalence of H- bonding interaction between benzyl alcohol with aniline and substituted aniline components.

2. Experimental section

2.1. Materials

The chemicals employed in this work have been of analytical grade. The purities of all the experimental liquids were analyzed by Gas Chromatography and the water content of samples were measured by Analab (Micro Aqua Cal 100) Karl Fischer Titrator and these were mentioned in Table S1. Further, the purity of chemical compounds was tested by comparison of densities (ρ) and speed of sound (u) measured in this work for pure compounds with literature values [14–39] were reported in Table S2.

2.2. Measurements

The analysis of densities were carried out with a Rudolph Research Analytical digital densimeter (DDH-2911 Model) equipped with a built-in solid state thermostat and a resident program with a temperature stability of ±0.02 K. The densities were automatically measured at the specified four temperatures by transferring the homogeneous and bubble free sample into the U-tube of the densimeter by using the medical syringe. The calibration of densimeter was performed at each specified temperature with air, de-ionized and double distilled water as standards and the detailed analysis procedure were previously reported [1,40]. The estimated uncertainty in density and excess volume was found to be $\pm 6 \times 10^{-5}$ gm. cm^{-3} and $\pm 0.003\ cm^3\ mol^{-1}$ respectively.

A multi frequency ultrasonic interferometer (M-82 Model, Mittal Enterprise, New Delhi, India) operated at 2 MHz, is used to measure the speed of sound, of the binary liquid mixtures at T = 303.15 K and T = 313.15 K by using a digital constant temperature water bath. The temperature stability was maintained within ±0.01 K by circulating thermostatic water bath around the cell with a circulating pump. In order to minimize the uncertainty of the measurement, several maxima were allowed to pass and their number (50) in the present study was counted. All maxima are recorded with the highest swing of the needle on the micrometre scale. The total distance d (cm) moved by the reflector is given by $d = n\lambda/2$, where λ is the wave length. The frequency, v, of the crystal being accurately known (2.0 MHz), the speed of sound, u in ms^{-1} is calculated by using the relation $u = v\lambda$. The details of analysis procedure have been previously reported [15,41]. The estimated uncertainty in speed of sound and excess isentropic compressibility values has been found to be $\pm 0.5\ m\ s^{-1}$ and $\pm 0.03\ T\ Pa^{-1}$respectively.

The FT-IR spectra of all pure and binary liquid mixtures had analyzed by using ALPHA FT-IR Spectrometer (Bruker, Germany). The samples were prepared by mixing of benzyl alcohol with aromatic amines in the 1:1 ratios. A drop of homogeneous sample has been placed to record the spectra in the region $4000–600\ cm^{-1}$ with $4.0\ cm^{-1}$ resolution. The same samples were measured by using JEOL RESONANCE JNM-ECS 400 ^{1}H NMR spectroscope operational at 400 MHz. In this NMR analysis of all samples containing $CDCl_3$ as an external solvent. All the experimental samples have been performed at room temperature.

2.3. Computational details

Gaussian 09 program suite [42] was used to perform all the optimization and frequency calculations of the complexes. The optimization and frequency calculations were accomplished using Moller-Plesset second order perturbation theory with B3LYP/6-311++G (d, p) level basis set. Interaction energies for all the optimized geometries were adjusted for the *Basis Set Superposition Error (BSSE)* utilizing Boys and Bernardi's counterpoise method

[43]. Furthermore, to determine strength of the intermolecular hydrogen bonds above said samples by using natural bond orbital (NBO) method [44] analysis. To better clarify the character of the H-bond interactions in numerous dimers of bond critical points (BCPs).

3. Results and discussion

3.1. Excess volumes (V^E)

The experimental densities and V^E values of the binary systems of benzyl alcohol with aniline and substituted aniline data were given in Table 1 and excess volumes (V^E) calculated by utilizing the following formula:

$$V^E \Big/ cm^3.mol^{-1} = [[X_1\ M_1 + X_2M_2]/\rho_m - [X_1M_1/\rho_1 + X_2M_2/\rho_2]] \quad (1)$$

where, X_1, X_2, M_1, M_2, $\rho_1$and ρ_2 are the mole fraction, molar mass and the density of pure liquid 1 and 2, respectively and ρ_m is density of the binary liquid mixtures. The uncertainty in excess volumes was of ±0.005 cm^3mol^{-1}.

The detail of curves in Fig. 1 at 303.15K indicate that the excess volume (V^E) data of benzyl alcohol with aniline and substituted anilines suggest that the property was negative entire composition range except for the system containing *N,N*-dimethylaniline (see Fig. 1).

Generally, the excess volume data of binary liquid systems perhaps influenced by the concerning ability of expansion and contraction of liquid components. If the factors accountable for expansion dominate the contributing contraction, V^E shows positive and contractive factors dominate the expansion factors, then V^E shows negative magnitude.

The constituent that cause contraction in volume are:

(a) intermolecular interactions arise among constituent atoms through the creation of Hydrogen bond.
(b) fit of complex of one constituent into the interstitial accommodation of the basic system of compounds of the another element
(c) structure of the molecule fitting with one another.

While, the factors that comprise expansion in volume may be attributed interms of

(a) declustering of the geometry of one or both of the component molecules in a solution.
(b) the geometry of molecular structures which does not allow the fitting of molecules of one component into the voids created by the molecules of second component.
(c) steric effect between benzyl alcohol with aniline and substituted anilines molecules.

A examination of V^E data in Fig. 1 reveal that responsible contraction in volume were dominant in the binary liquid mixtures containing of benzyl alcohol with aniline, N-methylaniline, *o*-chloroaniline and *m*-chloroaniline. But, the binary mixture of BA + NNDMA which has influenced by both contraction and expansion factors.

The negative V^E values of benzyl alcohol with the above said aromatic amines will follow the following order:

(BA + *o*-CA) > (BA + *m*-CA) > (BA + A) > (BA + NMA) > (BA + NNDMA)

Table 1
Mole fraction of benzyl alcohol (x_1), densities (ρ), experimental excess volumes (V^E) and predicted excess volumes (Redlich-Kister &Hwang) at T = 303.15 K–323.15 K and 0.1M Pa pressure for the binary mixtures of benzyl alcohol (1) with aniline, N-methylaniline, *N,N*-dimethylaniline, *o*-chloroaniline and *m*-chloroaniline (2).[a]

x_1	Density(ρ) ($g.cm^{-3}$)	V^E/cm^3mol^{-1}		
		Experimental	Redlich-Kister	Hwang
benzyl alcohol (1) with aniline (2)				
T = 303.15K				
0.0895	1.01586	−0.058	−0.057	−0.058
0.1810	1.01868	−0.093	−0.095	−0.095
0.2748	1.02137	−0.117	−0.117	−0.116
0.3709	1.02388	−0.125	−0.125	−0.124
0.4693	1.02628	−0.122	−0.123	−0.122
0.5701	1.02861	−0.113	−0.112	−0.113
0.6735	1.03085	−0.095	−0.094	−0.095
0.7796	1.03302	−0.07	−0.070	−0.070
0.8884	1.03514	−0.039	−0.039	−0.038
T = 308.15 K				
0.0895	1.01146	−0.031	−0.031	−0.031
0.1810	1.01415	−0.050	−0.051	−0.051
0.2748	1.01676	−0.063	−0.063	−0.063
0.3709	1.01929	−0.068	−0.068	−0.067
0.4693	1.02176	−0.067	−0.067	−0.066
0.5701	1.02417	−0.061	−0.061	−0.061
0.6735	1.02655	−0.052	−0.051	−0.052
0.7796	1.02888	−0.038	−0.038	−0.038
0.8884	1.03118	−0.021	−0.021	−0.021
T = 313.15 K				
0.0895	1.00717	−0.018	−0.018	−0.018
0.1810	1.00979	−0.030	−0.030	−0.030
0.2748	1.01236	−0.038	−0.038	−0.038
0.3709	1.01490	−0.043	−0.041	−0.041
0.4693	1.01736	−0.041	−0.042	−0.040
0.5701	1.01982	−0.039	−0.039	−0.039
0.6735	1.02224	−0.033	−0.034	−0.034
0.7796	1.02464	−0.025	−0.026	−0.026
0.8884	1.02703	−0.015	−0.015	−0.014
T = 318.15 K				
0.0895	1.00304	−0.015	−0.015	−0.015
0.1810	1.00568	−0.026	−0.026	−0.026
0.2748	1.00828	−0.033	−0.033	−0.033
0.3709	1.01083	−0.036	−0.036	−0.036
0.4693	1.01333	−0.035	−0.036	−0.034
0.5701	1.01583	−0.033	−0.033	−0.030
0.6735	1.01831	−0.029	−0.028	−0.028
0.7796	1.02074	−0.021	−0.020	−0.020
0.8884	1.02315	−0.010	−0.011	−0.010
T = 323.15 K				
0.0895	0.99907	−0.010	−0.010	−0.010
0.1810	1.00168	−0.017	−0.017	−0.017
0.2748	1.00427	−0.022	−0.021	−0.021
0.3709	1.00682	−0.024	−0.023	−0.024
0.4693	1.00935	−0.023	−0.023	−0.023
0.5701	1.01187	−0.022	−0.021	−0.021
0.6735	1.01435	−0.017	−0.018	−0.018
0.7796	1.01684	−0.013	−0.014	−0.013
0.8884	1.01933	−0.008	−0.008	−0.007
benzylalcohol (1) + *N*-methylaniline (2)				
T = 303.15 K				
0.1044	0.98767	−0.043	−0.043	−0.044
0.2078	0.99353	−0.076	−0.076	−0.075
0.3102	0.99929	−0.097	−0.096	−0.095
0.4116	1.00492	−0.105	−0.105	−0.104
0.5120	1.01045	−0.102	−0.102	−0.103
0.6115	1.01590	−0.091	−0.091	−0.092
0.7100	1.02126	−0.072	−0.072	−0.073
0.8076	1.02657	−0.047	−0.049	−0.048
0.9042	1.03188	−0.024	−0.023	−0.023
T = 308.15 K				
0.1044	0.98039	−0.027	−0.027	−0.028
0.2078	0.98648	−0.046	−0.045	−0.045
0.3102	0.99249	−0.055	−0.056	−0.055
0.4116	0.99845	−0.059	−0.059	−0.059
0.5120	1.00434	−0.056	−0.057	−0.057

(*continued on next page*)

Table 1 (*continued*)

x_1	Density(ρ) ($g.cm^{-3}$)	V^E/cm^3mol^{-1}		
		Experimental	Redlich-Kister	Hwang
0.6115	1.01022	−0.050	−0.050	−0.050
0.7100	1.01606	−0.041	−0.040	−0.040
0.8076	1.02185	−0.027	−0.027	−0.027
0.9042	1.02764	−0.013	−0.013	−0.013
T = 313.15 K				
0.1044	0.97687	−0.016	−0.016	−0.017
0.2078	0.98282	−0.028	−0.027	−0.028
0.3102	0.98873	−0.034	−0.034	−0.034
0.4116	0.99460	−0.037	−0.036	−0.036
0.5120	1.00043	−0.035	−0.035	−0.035
0.6115	1.00625	−0.031	−0.031	−0.031
0.7100	1.01202	−0.023	−0.024	−0.025
0.8076	1.01782	−0.017	−0.016	−0.016
0.9042	1.02358	−0.008	−0.008	−0.008
T = 318.15 K				
0.1044	0.97188	−0.013	−0.013	−0.013
0.2078	0.97793	−0.022	−0.022	−0.022
0.3102	0.98396	−0.028	−0.028	−0.028
0.4116	0.98997	−0.032	−0.031	−0.030
0.5120	0.99591	−0.029	−0.030	−0.029
0.6115	1.00187	−0.026	−0.026	−0.026
0.7100	1.00780	−0.020	−0.020	−0.020
0.8076	1.01373	−0.014	−0.013	−0.013
0.9042	1.01963	−0.006	−0.006	−0.006
T = 323.15 K				
0.1044	0.96724	−0.008	−0.008	−0.008
0.2078	0.97334	−0.013	−0.013	−0.013
0.3102	0.97941	−0.015	−0.016	−0.016
0.4116	0.98550	−0.019	−0.017	−0.017
0.5120	0.99154	−0.016	−0.016	−0.017
0.6115	0.99759	−0.014	−0.014	−0.014
0.7100	1.00364	−0.011	−0.011	−0.011
0.8076	1.00968	−0.007	−0.007	−0.007
0.9042	1.01572	−0.003	−0.003	−0.003
Benzyl alcohol (1) + *N*,*N*-dimethylaniline (2)				
T = 303.15 K				
0.1200	0.95718	−0.012	−0.013	−0.014
0.2348	0.96614	−0.018	−0.015	−0.015
0.3447	0.97499	−0.011	−0.009	−0.008
0.4501	0.98381	0.000	0.001	0.001
0.5511	0.99259	0.014	0.012	0.012
0.6481	1.00140	0.024	0.022	0.021
0.7412	1.01024	0.029	0.028	0.027
0.8308	1.01915	0.027	0.027	0.028
0.9170	1.02812	0.018	0.018	0.020
T = 308.15 K				
0.1200	0.95261	−0.009	−0.011	−0.012
0.2348	0.96164	−0.014	−0.012	−0.011
0.3447	0.97058	−0.008	−0.005	−0.004
0.4501	0.97948	0.004	0.005	0.006
0.5511	0.98835	0.018	0.016	0.016
0.6481	0.99724	0.029	0.026	0.024
0.7412	1.00619	0.032	0.031	0.030
0.8308	1.01520	0.029	0.029	0.029
0.9170	1.02428	0.019	0.020	0.021
T = 313.15 K				
0.1200	0.94878	−0.006	−0.007	−0.008
0.2348	0.95775	−0.007	−0.005	−0.004
0.3447	0.96664	0.002	0.002	0.004
0.4501	0.97550	0.014	0.013	0.013
0.5511	0.98436	0.025	0.023	0.023
0.6481	0.99326	0.032	0.032	0.031
0.7412	1.00216	0.036	0.036	0.035
0.8308	1.01116	0.031	0.033	0.033
0.9170	1.02019	0.022	0.021	0.023
T = 318.15K				
0.1200	0.94435	−0.004	−0.004	−0.005
0.2348	0.95335	−0.001	0.000	0.000
0.3447	0.96230	0.008	0.009	0.010
0.4501	0.97122	0.021	0.020	0.021
0.5511	0.98015	0.032	0.031	0.031
0.6481	0.98910	0.040	0.039	0.038
0.7412	0.99809	0.042	0.042	0.041

Table 1 (*continued*)

x_1	Density(ρ) ($g.cm^{-3}$)	V^E/cm^3mol^{-1}		
		Experimental	Redlich-Kister	Hwang
0.8308	1.00716	0.037	0.037	0.038
0.9170	1.01631	0.024	0.024	0.025
T = 323.15K				
0.1200	0.94048	−0.001	−0.001	−0.003
0.2348	0.94947	0.003	0.004	0.004
0.3447	0.95843	0.012	0.013	0.014
0.4501	0.96735	0.025	0.024	0.025
0.5511	0.97628	0.036	0.035	0.034
0.6481	0.98525	0.043	0.043	0.042
0.7412	0.99424	0.046	0.045	0.045
0.8308	1.00334	0.039	0.040	0.041
0.9170	1.01249	0.026	0.026	0.027
Benzyl alcohol (1) + *o*- chloroaniline (2)				
T = 303.15 K				
0.1018	1.18836	−0.225	−0.226	−0.226
0.2031	1.17395	−0.419	−0.417	−0.417
0.3041	1.15894	−0.563	−0.561	−0.561
0.4047	1.14331	−0.652	−0.651	−0.652
0.5049	1.12698	−0.679	−0.682	−0.682
0.6047	1.11007	−0.651	−0.653	−0.653
0.7041	1.09258	−0.566	−0.565	−0.564
0.8031	1.07451	−0.422	−0.421	−0.421
0.9017	1.05600	−0.230	−0.230	−0.231
T = 308.15 K				
0.1018	1.18305	−0.173	−0.173	−0.173
0.2031	1.16826	−0.323	−0.322	−0.322
0.3041	1.15300	−0.434	−0.435	−0.435
0.4047	1.13727	−0.503	−0.505	−0.505
0.5049	1.12104	−0.526	−0.528	−0.528
0.6047	1.10431	−0.503	−0.502	−0.502
0.7041	1.08709	−0.431	−0.430	−0.430
0.8031	1.06949	−0.319	−0.316	−0.316
0.9017	1.05153	−0.168	−0.169	−0.169
T = 313.15 K				
0.1018	1.17805	−0.133	−0.133	−0.133
0.2031	1.16288	−0.244	−0.244	−0.243
0.3041	1.14735	−0.326	−0.326	−0.326
0.4047	1.13148	−0.377	−0.377	−0.377
0.5049	1.11521	−0.391	−0.394	−0.394
0.6047	1.09862	−0.374	−0.376	−0.375
0.7041	1.08173	−0.326	−0.324	−0.324
0.8031	1.06451	−0.244	−0.241	−0.241
0.9017	1.04700	−0.130	−0.131	−0.131
T = 318.15 K				
0.1018	1.17274	−0.098	−0.098	−0.098
0.2031	1.15737	−0.179	−0.179	−0.179
0.3041	1.14176	−0.241	−0.240	−0.240
0.4047	1.12589	−0.279	−0.277	−0.277
0.5049	1.10970	−0.288	−0.290	−0.290
0.6047	1.09331	−0.276	−0.277	−0.277
0.7041	1.07667	−0.239	−0.240	−0.240
0.8031	1.05984	−0.182	−0.180	−0.180
0.9017	1.04277	−0.099	−0.099	−0.099
T = 323.15 K				
0.1018	1.16793	−0.077	−0.079	−0.079
0.2031	1.15255	−0.149	−0.145	−0.145
0.3041	1.13687	−0.196	−0.195	−0.195
0.4047	1.12103	−0.228	−0.225	−0.225
0.5049	1.10491	−0.234	−0.235	−0.235
0.6047	1.08860	−0.222	−0.224	−0.224
0.7041	1.07212	−0.191	−0.193	−0.193
0.8031	1.05547	−0.142	−0.143	−0.143
0.9017	1.03870	−0.079	−0.078	−0.078
Benzyl alcohol (1) + *m*- chloroaniline (2)				
T = 303.15 K				
0.1021	1.18969	−0.082	−0.082	−0.082
0.2037	1.17342	−0.144	−0.144	−0.144
0.3048	1.15694	−0.186	−0.188	−0.188
0.4055	1.14031	−0.213	−0.213	−0.213
0.5057	1.12348	−0.220	−0.219	−0.219
0.6054	1.10648	−0.207	−0.207	−0.207
0.7048	1.08933	−0.179	−0.178	−0.178
0.8036	1.07205	−0.133	−0.133	−0.133

Table 1 (*continued*)

x_1	Density(ρ) (g.cm^{-3})	V^E/cm^{3}mol^{-1}		
		Experimental	Redlich-Kister	Hwang
0.9020	1.05466	−0.073	−0.073	−0.073
T = 308.15 K				
0.1021	1.18495	−0.063	−0.063	−0.063
0.2037	1.16865	−0.114	−0.113	−0.113
0.3048	1.15215	−0.146	−0.148	−0.148
0.4055	1.13557	−0.169	−0.169	−0.169
0.5057	1.11882	−0.174	−0.174	−0.174
0.6054	1.10195	−0.165	−0.165	−0.165
0.7048	1.08496	−0.143	−0.142	−0.142
0.8036	1.06786	−0.106	−0.105	−0.105
0.9020	1.05079	−0.057	−0.057	−0.057
T = 313.15 K				
0.1021	1.18024	−0.047	−0.047	−0.047
0.2037	1.16379	−0.081	−0.082	−0.082
0.3048	1.14727	−0.106	−0.105	−0.105
0.4055	1.13063	−0.119	−0.118	−0.118
0.5057	1.11394	−0.124	−0.122	−0.122
0.6054	1.09712	−0.114	−0.118	−0.118
0.7048	1.08030	−0.104	−0.104	−0.104
0.8036	1.06340	−0.080	−0.081	−0.081
0.9020	1.04644	−0.047	−0.046	−0.047
T = 318.15 K				
0.1021	1.17553	−0.028	−0.029	−0.029
0.2037	1.15909	−0.055	−0.053	−0.053
0.3048	1.14257	−0.073	−0.071	−0.070
0.4055	1.12595	−0.080	−0.081	−0.081
0.5057	1.10934	−0.085	−0.084	−0.083
0.6054	1.09263	−0.077	−0.079	−0.079
0.7048	1.07588	−0.065	−0.067	−0.067
0.8036	1.05913	−0.048	−0.049	−0.049
0.9020	1.04237	−0.027	−0.026	−0.026
T = 323.15 K				
0.1021	1.17090	−0.016	−0.015	−0.015
0.2037	1.15436	−0.026	−0.027	−0.027
0.3048	1.13782	−0.034	−0.035	−0.035
0.4055	1.12126	−0.039	−0.039	−0.039
0.5057	1.10471	−0.041	−0.040	−0.040
0.6054	1.08814	−0.039	−0.038	−0.039
0.7048	1.07154	−0.034	−0.033	−0.033
0.8036	1.05496	−0.025	−0.025	−0.025
0.9020	1.03837	−0.014	−0.014	−0.014

[a] The standard uncertainties are $u\ (x_1) = 1 \times 10^{-4}$, $u\ (\rho) = 2 \times 10^{-5}$ g cm^{-3}, $u\ (T) = 0.01$ K for density, $u\ (p) = 1$ kPa, and u $(V^E) = \pm 0.005$ cm^3 mol^{-1}.

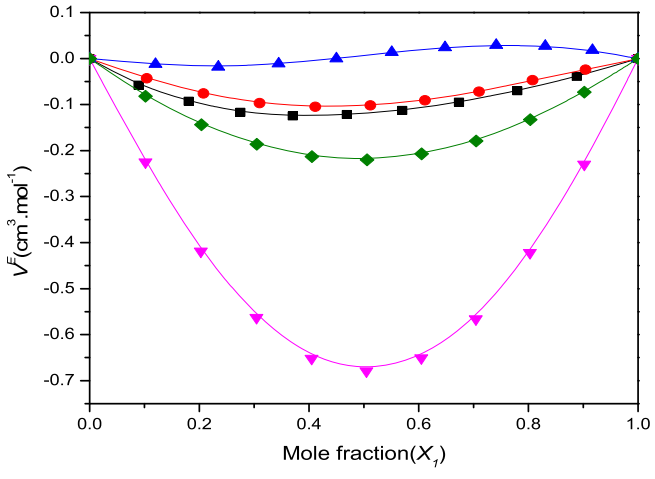

Fig. 1. Variation of excess volume (V^E) of the binary liquid mixture of benzylalcohol (1) with aniline (2) (■), N-methylaniline (2) (●), *N,N*-dimethylaniline (2) (▲), *o*-chloroaniline (2) (▼), *m*-chloro aniline (2) (◆) at 303.15 K.

Therefore, the strength of molecular interaction between benzyl alcohol with amines decreases from *o*-chloroaniline to *N,N*-dimethylaniline. This can be explained by taking into the following considerations.

The solvent-solute interaction in ortho chloro aniline has more than the meta chloro aniline due to polar nature more in ortho isomer [30,36]. Further, V^E data of the two isomers of chloroanilines suggests that stronger interactions are prevailing in *o*-chloroaniline when compared to *m*-chloroaniline. Since in the case of *m*-chloroaniline, the chlorine atom was offered by steric hindrance with $-NH_2$ group and in the case of *o*-chloroaniline, the chlorine atom was very close to $-NH_2$ group and hence, the overall interactions are stronger when compared to *m*-chloroaniline.

The results of the thermodynamic parameters of the above said liquids point out that the solvent-solute inter molecular interaction increases with the strength of base, the dissociation constants (P^K) of alkyl substituted aryl amines are: aniline (P^{Kb} =9.38), N-methylaniline (P^{Kb} =9.16), *N,N*-dimethylaniline (P^{Kb} =8.32) K existence the ionization constant of the comparing anilinium ions gives to $RNH_3^+ \rightleftarrows RNH_2 + H^+$ [45–47]. From Fig. 1, it is clearly evident that the strength of hydrogen bonding formation decreases from aniline to *N,N*-dimethylaniline. 1° and 2° - amines were formed intermolecular interaction through H- bonding between nitrogen atom of one molecule and hydrogen atom of another molecule. From V^E results, the intermolecular interaction was more in 1° - amines than in 2^0- amines because two H- atoms form hydrogen bond formation in it. Tertiary amines(*N,N*-dimethylaniline) do not exhibit intermolecular interaction due to the absence of H- atom and the non-existence of intermolecular hydrogen bonding O-H ····N bond and this can be clearly observed from the FT-IR spectra of benzyl alcohol + *N,N*-dimethylaniline mixture. The negative V^E data at $x_1 = 0.3447$ is −0.011 cm^3 mol^{-1} due to the net packing effect. The inductive, solvation and steric effects of the alkyl group of aryl amines are responsible for the sign and magnitude of excess volume in the present investigated systems.

The binary systems of benzyl alcohol with *o*-chloroaniline (P^{Kb}=11.34) and *m*-chloroaniline (P^{Kb}=10.48), the former will exhibit more negative V^E (-0.125 cm^3 mol^{-1}) at 303.15K than latter. In the case of *o*-chloroaniline the chlorine isomer was placed nearer to the -NH_2 group, where as in *m*-chloroaniline the position of chlorine isomer is shifted to its next position and the chlorine isomer (-Cl) is offering to steric hindrance with -NH_2 group of chloroaniline molecule. As the separation of chloro group from *ortho* position to *meta* position, the distance between $-NH_2$ group and chloro group increases thereby inter molecular interactions are weak/less in the system containing *m*-chloroaniline. This contraction in molar volume (V^E) shows negative magnitude.

3.2. Excess isentropic compressibilities (κ_s^E)

The mole fraction (x_i) of benzyl alcohol, the experimental density (ρ), speed of sound (u), isentropic compressibility (κ_s) and excess isentropic compressibility (κ_s^E) for the binary systems of benzyl alcohol with aniline and substituted anilines at 303.15K and 313.15K were incorporated in Table 2 and the κ_s^E values were diagrammatically represented in Fig. 2. A detailed description regarding reckoning of κ_s^E was already described earlier [15]. Moreover, the experimental κ_s^E results were fitted into Redlich-Kister equation and Hwang et al. equations (2) and (3) for all the investigated systems. The experimental speeds of sound (u) data were analyzed interms of CFT [11] and FLT [12,13] to check their capability were also given in Table 2.

Table 2
Mole fraction (x_1) of benzyl alcohol, experimental sound speed(u), isentropic compressibilities (κ_s), excess isentropic compressibilities (κ_s^E) and predicted excess isentropic compressibilities (Redlich-Kister& Hwang equations) theoretical sound speed data of (FLT and CFT) benzylalcohol (1) with aniline, N-methylaniline, *N,N*-dimethylaniline, *o*-chloroaniline, *m*-chloroaniline (2) at 303.15K and 313.15 K and 0.1M Pa pressure.[a]

x_1	u(exp) (m.s^{-1})	κ_s (TPa^{-1})	u_{FLT}	u_{CFT}	κ_s^E/(TPa^{-1})		
			(m.s^{-1})		Experimental	Redlich-Kister	Hwang
benzyl alcohol (1) + aniline (2)							
T = 303.15 K							
0.0895	1605.7	381.80	1610.7	1605.6	−1.12	−1.11	−1.10
0.1810	1596.1	385.34	1603.9	1596.1	−1.93	−1.95	−1.95
0.2748	1586.4	389.06	1595.9	1586.4	−2.55	−2.57	−2.57
0.3709	1576.5	392.97	1586.2	1576.4	−2.96	−2.98	−2.98
0.4693	1566.6	397.03	1575.4	1566.2	−3.23	−3.19	−3.19
0.5701	1556.3	401.39	1564.1	1555.9	−3.18	−3.18	−3.18
0.6735	1545.9	405.92	1551.9	1545.3	−2.95	−2.95	−2.95
0.7796	1535.2	410.73	1539.1	1534.4	−2.44	−2.41	−2.41
0.8884	1523.9	415.99	1525.9	1523.3	−1.46	−1.47	−1.48
T = 313.15 K							
0.0895	1570.1	402.8	1570.6	1569.7	−1.03	−1.03	−1.03
0.1810	1561.9	405.9	1562.7	1561.3	−1.83	−1.84	−1.84
0.2748	1553.5	409.3	1554.3	1552.7	−2.45	−2.45	−2.45
0.3709	1544.9	412.8	1545.6	1543.9	−2.88	−2.85	−2.85
0.4693	1536.0	416.6	1536.3	1535.0	−3.05	−3.05	−3.05
0.5701	1526.9	420.6	1527.0	1525.8	−3.04	−3.04	−3.03
0.6735	1517.5	424.8	1517.3	1516.4	−2.76	−2.78	−2.78
0.7796	1507.8	429.3	1507.4	1506.8	−2.22	−2.24	−2.24
0.8884	1497.7	434.1	1497.4	1497.0	−1.35	−1.34	−1.34
benzyl alcohol (1)+ N- methylaniline (2)							
T = 303 .15 K							
0.1044	1545.0	424.2	1548.8	1545.1	−1.73	−1.71	−1.71
0.2078	1540.9	423.9	1547.8	1541.3	−2.99	−3.02	−3.02
0.3102	1537.1	423.6	1545.8	1537.5	−3.89	−3.93	−3.93
0.4116	1533.3	423.3	1542.8	1533.8	−4.40	−4.44	−4.44
0.5120	1529.6	423.0	1538.9	1530.1	−4.53	−4.55	−4.55
0.6115	1526.1	422.7	1534.3	1526.4	−4.34	−4.29	−4.29
0.7100	1522.5	422.4	1528.9	1522.7	−3.75	−3.67	−3.67
0.8076	1518.8	422.3	1523.2	1519.1	−2.72	−2.72	−2.72
0.9042	1515.3	422.1	1517.6	1515.5	−1.47	−1.49	−1.49
T = 313.15 K							
0.1044	1507.9	450.7	1509.4	1508.5	−1.54	−1.55	−1.55
0.2078	1505.2	449.5	1507.7	1506.0	−2.84	−2.82	−2.82
0.3102	1502.6	448.3	1505.7	1503.6	−3.74	−3.74	−3.74
0.4116	1500.1	447.1	1503.4	1501.2	−4.25	−4.27	−4.27
0.5120	1497.7	445.9	1500.8	1498.7	−4.39	−4.41	−4.41
0.6115	1495.3	444.7	1498.2	1496.4	−4.13	−4.14	−4.14
0.7100	1493.0	443.4	1495.3	1494.0	−3.52	−3.51	−3.51
0.8076	1490.8	442.2	1492.6	1491.6	−2.59	−2.56	−2.56
0.9042	1488.7	440.9	1489.7	1489.3	−1.35	−1.36	−1.36
benzyl alcohol (1) + *N,N*-di methylaniline (2)							
T = 303.15 K							
0.1200	1475.2	480.1	1474.5	1475.0	−2.03	−2.03	−2.02
0.2348	1480.2	472.4	1478.8	1479.9	−3.55	−3.51	−3.51
0.3447	1484.8	465.2	1482.3	1484.5	−4.44	−4.47	−4.48
0.4501	1489.2	458.3	1485.6	1488.9	−4.88	−4.95	−4.95
0.5511	1493.5	451.7	1488.8	1493.1	−4.95	−4.99	−4.98
0.6481	1497.6	445.2	1492.3	1497.2	−4.64	−4.62	−4.62
0.7412	1501.5	439.1	1496.2	1501.1	−3.97	−3.90	−3.90
0.8308	1505.1	433.1	1500.8	1504.9	−2.90	−2.86	−2.86
0.9170	1508.5	427.4	1506.0	1508.5	−1.52	−1.55	−1.55
T = 313.15 K							
0.1200	1438.0	509.7	1437.4	1438.6	−1.95	−1.95	−1.95
0.2348	1443.8	500.9	1442.7	1444.9	−3.34	−3.30	−3.30
0.3447	1449.3	492.5	1447.5	1450.9	−4.11	−4.14	−4.15
0.4501	1454.8	484.4	1452.1	1456.7	−4.50	−4.54	−4.54
0.5511	1460.3	476.4	1456.8	1462.2	−4.56	−4.56	−4.56
0.6481	1465.7	468.7	1461.9	1467.6	−4.24	−4.23	−4.22
0.7412	1471.1	461.1	1467.1	1472.7	−3.61	−3.58	−3.58
0.8308	1476.4	453.7	1473.1	1477.7	−2.66	−2.65	−2.65
0.9170	1481.7	446.5	1479.5	1482.4	−1.44	−1.45	−1.45
benzyl alcohol (1) + *o*- chloroaniline (2)							
T = 303.15 K							
0.1018	1470.9	388.9	1489.5	1472.7	−0.83	−0.83	−0.83
0.2031	1474.4	391.8	1509.2	1477.4	−1.69	−1.65	−1.65
0.3041	1478.0	395.0	1525.3	1482.0	−2.27	−2.32	−2.32
0.4047	1482.1	398.2	1537.3	1486.5	−2.74	−2.76	−2.76
0.5049	1486.4	401.6	1544.2	1490.9	−2.91	−2.92	−2.92
0.6047	1490.9	405.3	1546.4	1495.3	−2.79	−2.78	−2.78

Table 2 (*continued*)

x_1	u(exp) (m.s^{-1})	κ_s (TPa^{-1})	u_{FLT} (m.s^{-1})	u_{CFT}	κ_s^E/(TPa^{-1})		
					Experimental	Redlich-Kister	Hwang
0.7041	1495.6	409.2	1544.0	1499.5	−2.38	−2.36	−2.36
0.8031	1500.6	413.3	1536.7	1503.8	−1.71	−1.70	−1.70
0.9017	1506.0	417.5	1525.6	1507.9	−0.87	−0.88	−0.88
T = 313.15 K							
0.1018	1440.8	408.9	1451.0	1442.3	−0.61	−0.65	−0.64
0.2031	1445.4	411.6	1463.7	1447.6	−1.43	−1.37	−1.37
0.3041	1450.2	414.4	1474.5	1452.8	−2.08	−2.00	−2.00
0.4047	1455.0	417.5	1483.2	1457.9	−2.45	−2.44	−2.44
0.5049	1459.9	420.7	1489.3	1462.9	−2.56	−2.61	−2.61
0.6047	1464.9	424.2	1493.2	1467.9	−2.43	−2.50	−2.50
0.7041	1470.1	427.7	1494.9	1472.7	−2.11	−2.12	−2.12
0.8031	1475.4	431.5	1494.1	1477.6	−1.52	−1.51	−1.51
0.9017	1481.0	435.5	1491.0	1482.3	−0.78	−0.77	−0.77
benzyl alcohol (1) + *m*- chloroaniline (2)							
T = 303.15 K							
0.1021	1515.4	366.0	1522.2	1515.9	−1.00	−1.00	−0.99
0.2037	1514.9	371.3	1526.8	1515.7	−1.82	−1.83	−1.83
0.3048	1514.5	376.8	1529.8	1515.4	−2.45	−2.45	−2.45
0.4055	1514.1	382.5	1531.7	1515.1	−2.87	−2.85	−2.86
0.5057	1513.7	388.5	1531.9	1514.7	−3.03	−3.02	−3.02
0.6054	1513.3	394.6	1530.4	1514.3	−2.92	−2.93	−2.93
0.7048	1512.9	401.1	1527.8	1513.8	−2.57	−2.59	−2.59
0.8036	1512.6	407.7	1523.6	1513.3	−1.99	−1.99	−1.99
0.9020	1512.3	414.6	1518.3	1512.7	−1.13	−1.13	−1.13
T = 313.15 K							
0.1021	1484.3	384.6	1487.7	1484.6	−0.96	−0.96	−0.95
0.2037	1484.6	389.9	1490.5	1485.1	−1.71	−1.72	−1.72
0.3048	1484.9	395.3	1492.6	1485.5	−2.28	−2.27	−2.28
0.4055	1485.2	401.0	1493.9	1485.9	−2.63	−2.62	−2.63
0.5057	1485.5	406.8	1494.6	1486.3	−2.78	−2.77	−2.77
0.6054	1485.8	412.9	1494.1	1486.5	−2.68	−2.70	−2.69
0.7048	1486.1	419.1	1493.7	1486.7	−2.40	−2.40	−2.39
0.8036	1486.4	425.6	1492.2	1486.9	−1.85	−1.86	−1.86
0.9020	1486.7	432.4	1490.2	1487.0	−1.07	−1.07	−1.07

[a] The standard uncertainties are $u(X_1) = 1 \times 10^{-4}$, $u(u) = 0.3\%$, $u(T) = 0.02$ K for speed of sound and $u(p) = 1$ kPa.

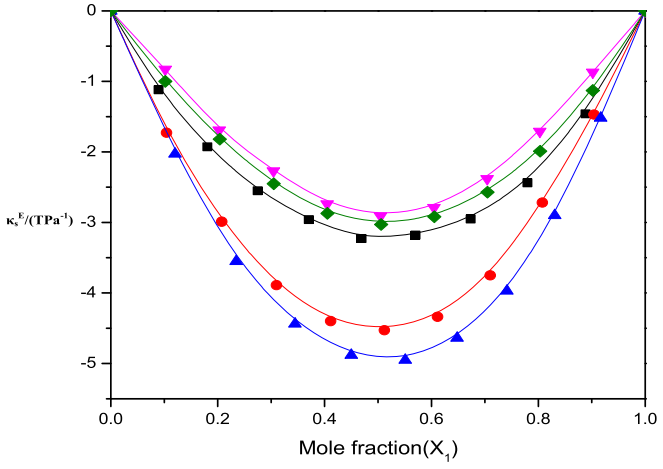

Fig. 2. Variation of excess isentropic compressibility (κ_s^E) of the binary liquid mixture of benzylalcohol (1) with aniline (2) (■), N-methylaniline (2) (●), *N,N*-di methylaniline (2) (▲), *o*- chloroaniline (2) (▼), *m*- chloroaniline (2) (◆) at 303.15 K.

The isentropic compressibility (κ_S) as follows [48,49]:

$$\kappa_S = u^{-2}\rho^{-1} \tag{2}$$

The comparable excess isentropic compressibilities (κ_S^E) have been calculated from the subsequent equation:

$$\kappa_S^E = \kappa_S - \kappa_S^{id} \tag{3}$$

where κ_s^{id} is the ideal value of the isentropic compressibility and calculated by using Benson and Kiyohara [50] expression was given below:

$$\kappa_s^{id} = \sum_{i=1}^{2} \varphi_i \left[\kappa_{s,i} + TV_i\left(\alpha_i^2\right)/C_{p,i}\right] - \left\{T\left(\sum_{i=1}^{2} x_i V_i\right)\left(\sum_{i=1}^{2} \varphi_i \alpha_i\right)^2 \Big/ \sum_{i=1}^{2} x_i C_{p,i}\right\} \tag{4}$$

where, C_{pi} and α_i are the molar heat capacity and the thermal expansion coefficient of the *i*th component respectively. The value of C_{pi} was obtained and evaluated from literature [41,51,52]. The thermal expansion coefficient α_i was calculated by following equation (5) [53].

$$\alpha = -\frac{1}{\rho}\left(\frac{\partial \rho}{\partial T}\right)_p \tag{5}$$

The sign and magnitude of κ_s^E plays a key role within the estimation of molecular interaction among pure components and their mixtures. Moreover, it has been suggested by Kiyohara and Benson [52] that κ_s^E data is the factors of several opposing effects. The strong intermolecular interactions between molecules could arise interms of charge exchange, dipole-induced dipole and dipole-dipole associations, interstitial convenience, formation of H- bonding contributing negative κ_s^E values, while dissociation of liquid order structure causes to positive excess isentropic compressibility. Hence the magnitude and sign of different kinds mainly rely on the molecular nature of component liquids.

A perusal of curves in Fig. 2 reveal that the more negative κ_S^E records additionally reveal that liquid combinations of benzyl alcohol with *N,N*-dimethyl aniline are less compressible than the comparing ideal mixtures [54] and also the remaining mixtures namely N-methyl aniline, aniline, *m*-chloroaniline, *o*-chloroaniline. Moreover, liquids of dissimilar molecular size and shape in general combine with a decrease in volume leading to negative κ_S^E values. Further, the κ_S^E data in Table 2 reveals that the property is ideal in all the binary liquid mixtures of benzyl alcohol with aniline and substituted anilines. Since the molar volume of all the pure liquids at 303.15 K are: BA ($104.26\ cm^3\ mol^{-1}$), A ($91.95\ cm^3\ mol^{-1}$), NMA ($109.15\ cm^3\ mol^{-1}$), NNDMA ($127.80\ cm^3\ mol^{-1}$), *o*-CA ($106.12\ cm^3\ mol^{-1}$), *m*-CA ($108.83\ cm^3\ mol^{-1}$),.Since, the molar volume data of NNDMA is more when compared with molar volumes of the other component molecules indicate that a more efficient packing occurred when BA and NNDMA molecules were combined, which inturn may be responsible for more negative κ_S^E data were observed in NNDMA system.

The algebraic values of κ_S^E for the mixtures of benzyl alcohol with the above said aromatic amines will follow the following order:

(BA + NNDMA)> (BA + NMA)> (BA + A)> (BA + *m*-CA)> (BA + *o*-CA).

The κ_S^E values are negative over the whole mole fraction range at 303.15K and 313.15K temperatures, indicating the predominance of interstitial accommodation of the component molecule effect and this may be ascribed to the relative strength between component molecules as defined in the literature [55,56]. Finally, it is concluded that excess volume and excess isentropic compressibilities data are negative in all the systems and the property decreases with increasing of the temperature. This may be due to on increasing temperature, more thermal de-clustering of self-association than cross-association of component molecules of mixture and resulting greater fitting of voids of one component molecule into another.

Experimental speeds of sound were examined with the help of CFT [11], FLT [12,13] and these values given in Table 2. An analysis between experimental and theoretical speed of sound values suggest that CFT gives good approximation and given in Table S3. These theories had analysed with relative root mean deviation (RMSD) and mean percentage deviation (MPD) by utilizing the fallowing equations.

$$RMSD = \left[\frac{1}{n}\sum_{i=1}^{n}\left[\frac{y_{exp} - y_{cal}}{y_{exp}}\right]^2\right]^{1/2} \tag{6}$$

$$MPD = \frac{100}{N}\sum_{i=1}^{N}\left|\frac{\left(y_i^{cal} - y_i^{exp}\right)}{y_i^{exp}}\right| \tag{7}$$

The experimental data (V^E) and κ_S^E data were computed in terms of Redlich-Kister [57] and Hwang et al. [58] equations and these values given in Table 1. The method of correlation of excess properties with Redlich-Kister and Hwang et al. equations and relative standard deviation $\sigma(X^E)$ were reported previously [1]. The relative standard deviation $\sigma(X^E)$ values are given in Table S4 and S5. An examination of $\sigma(X^E)$ values recommend that Redlich-Kister & Hwang equation give good estimation both in V^E, and κ_S^E of binary liquid mixtures. The absolute values of both V^E/κ_S^E decrease with increasing the temperature in all the binary mixtures indicating that thermal energy reduces the molecular association between unlike molecules. Thermodynamic investigations have been elucidating interms of intermolecular hydrogen bond existence in the binary liquid mixtures and these were further affirmed by FT-IR and ^{1}HNMR investigations.

3.3. Experimental details of FT-IR studies

The Infrared spectra of a molecule (solute-solvent) depends not just on the strength of the bond amongst solute and solvent, however may also be extraordinarily influenced by ecological elements [59]. FT-IR spectral changes are widely employed in study of intermolecular H- bonding existence between the binary liquid mixture of benzyl alcohol and aniline, N-methylaniline, *N,N*-dimethylaniline, *o*-chloroaniline, *m*-chloroaniline. The measurement of spectroscopic studies of solute - solvent interactions; particularly hydrogen-bond interactions between binary liquid mixtures of excessive shifts of O-H stretching in hydrogen bond donor solvent (benzyl alcohol) and of −NH stretching in Hydrogen Bond Acceptor solvents (aniline, N-methylaniline, *o*-chloroaniline, *m*-chloroaniline) leads to formation of hydrogen-bonding was observed. But in the binary mixture containing benzyl alcohol with *N,N*-dimethylaniline less solute/solvent interactions was observed and the strength of hydrogen bonding interaction less than the other liquid mixtures. This was clearly observed interms of chemical shift value which was incorporated in Table 3.

Moreover, a perusal of FT-IR data in Table 3 and Figs. 3 and 4 for all the pure liquids and their equimolar binary mixture systems of the frequencies clearly indicate that the studied binary mixtures have H-bonding interaction between amine and hydroxyl functional groups (except *N,N*-dimethylaniline). The pure liquids shows that broad band in the 3600-3200 cm^{-1} range (hydrogen bonded −OH stretching) [60]. The experimental FT-IR spectrum of the pure components resultant absorption bands, namely aniline (two peaks at 3433 cm^{-1}, 3356 cm^{-1}), N-methylaniline (one peak at 3411 cm^{-1}), *N,N*-dimethylaniline (no peak), *o*-chloroaniline (two peaks at 3466 cm^{-1}, 3373 cm^{-1}) and *m*-chloroaniline (two peaks at 3455 cm^{-1},3368 cm^{-1}) of amine functional group and benzyl alcohol show broad band −OH stretching at 3320 cm^{-1}. Further, the resultant absorption bands of binary liquid frequencies are, benzyl alcohol + aniline = 3354 cm^{-1}, benzyl alcohol + N-methylaniline = 3347 cm^{-1}), benzyl alcohol + *N,N*-dimethylaniline = 3343(broad peak), benzyl alcohol + *o*-chloroaniline = 3368 cm^{-1}) and benzyl alcohol + *m*-chloroaniline = 3357 cm^{-1} given in Table 3 and shown in Figs. 3 and 4. The values of the O-H stretching frequency have been used as a best elucidation of the strength of hydrogen bonding between “free” O-H stretching frequencies of the spectra of benzyl alcohol in aromatic amines. The variation in $\Delta\nu$ values suggest that the strength of the H- bond interaction depends on the electron density on the oxygen atom of the O-H group.

Finally, the experimental data of FT-IR Spectroscopy suggest that, the existence of the strong hydrogen bond between benzyl alcohol and *o*-chloroaniline liquid mixture due to longer the OH bond, thereby shift the band to higher frequency change. It's to be expected as a result of the influence of chlorine on the polarization of NH_2 group within the *o*-chloroaniline. The electron density of *o*-chloroaniline decrease on nitrogen in NH_2 group due to influence of chlorine group due to the formation of a stronger H- bond between benzyl alcohol and *o*-chloroaniline. In *o, m*-chloroaniline compounds containing NH_2 group, and chlorine atom to form both intermolecular and intramolecular hydrogen bond. Weak H-bonding is influence in the binary systems of benzyl alcohol with N-methylaniline leading to shift the O-H band to lower frequency change. But benzyl alcohol with *N,N*-dimethylaniline frequency change due to lone pair electron on N-atom of *N,N*-dimethylaniline.

Table 3
Experimental FT-IR analysis of the pure and equimolar binary mixture systems at temperature T = 298.15 K.

Compound	Band	Experimental	
		ν (c.m^{-1})	$\Delta\nu$ (c.m^{-1})
benzyl alcohol	OH	3320 (broad, s)	–
Aniline	NH_2 (1^0-amine)(two peaks)	(i) 3433 (w) (ii) 3356(m)	–
N-methyl aniline	NH (2^0-amine) (one peak)	3411(m)	–
N,N-dimethyl aniline	N (3^0-amine) (no peak)	–	–
o-chloroaniline	NH_2 (1^0-amine) (two peaks)	(i) 3466(w) (ii) 3373(m)	–
m-chloroaniline	NH_2 (1^0-amine) (two peaks)	(i) 3455(w) (ii) 3368(m)	–
Shift in wavenumbers with respect to benzyl alcohol and anilines [a]			
benzyl alcohol + aniline	OH – NH_2	3354	34 (−79 (w),-2 (m))[a]
benzyl alcohol + N-methyl aniline	OH – NH	3347	27 (−64 (m))[a]
benzyl alcohol + *N,N*-dimethyl aniline	OH – N	3343	23 (no peak)[a]
benzyl alcohol + *o*-chloroaniline	OH – NH_2	3368	48 (−98(w),-5(m))[a]
Benzyl alcohol + *m*-chloroaniline	OH – NH_2	3357	37 (−98(w),-11(m)[a]

[a] Bracket shows change of frequencies of mixtures with respect to aniline peak frequencies.

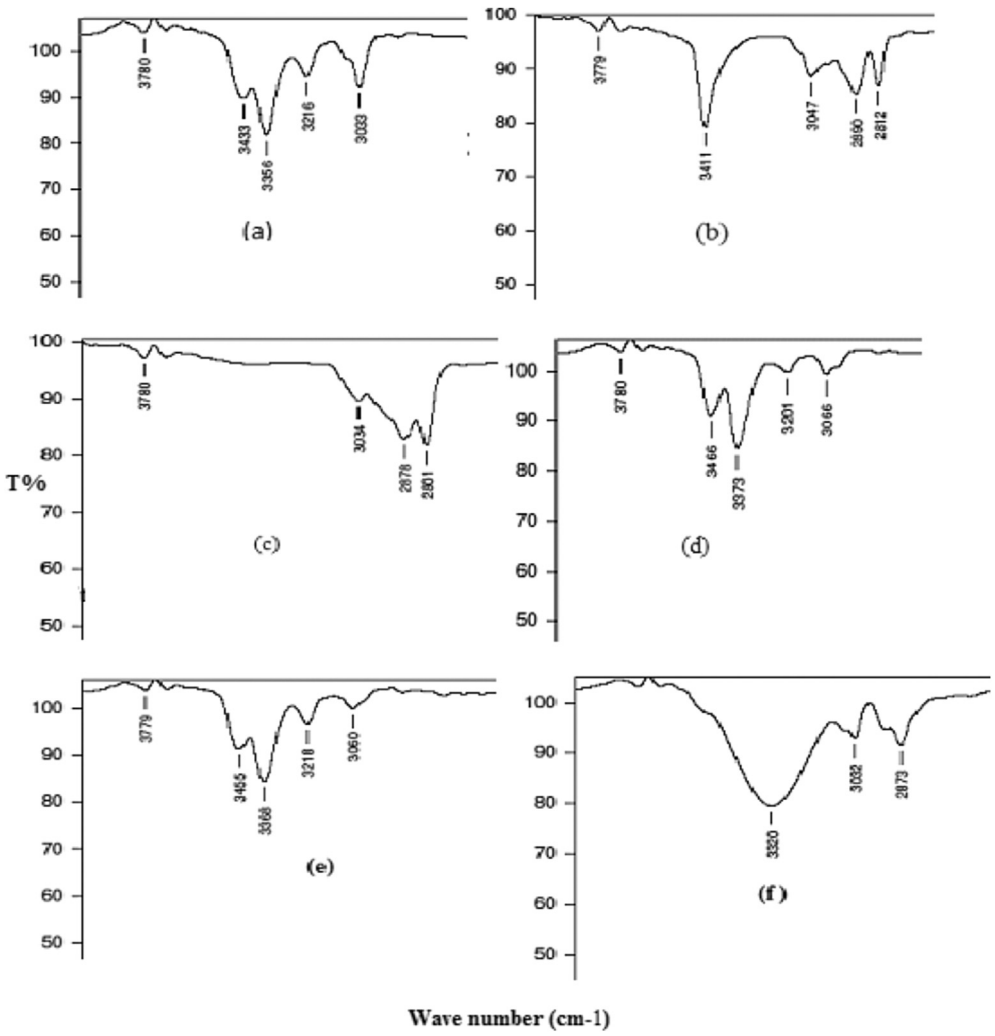

Fig. 3. FT-IR spectra of Pure components: aniline (a), N-methylaniline (b), *N,N*-dimethylaniline (c), *o*-chloroaniline (d), *m*-chloro aniline (e), benzyl alcohol (f).

3.4. ^{1}H NMR spectroscopy studies: [hydrogen bonding effects on chemical shifts − OH and NH protons]

The chemical shifts of alcohol functional group OH and amine functional group of 1°, 2°, 3° protons vary over a wide range pivot on details of sample preparation and substrate structure. From Table 4, the shifts are firmly influenced by hydrogen bonding, with strong downfield shifts of H-bonded groups of binary liquid mixtures compared to free OH and NH groups of pure liquids. Thus NH signals tend to move downfield with respect components because

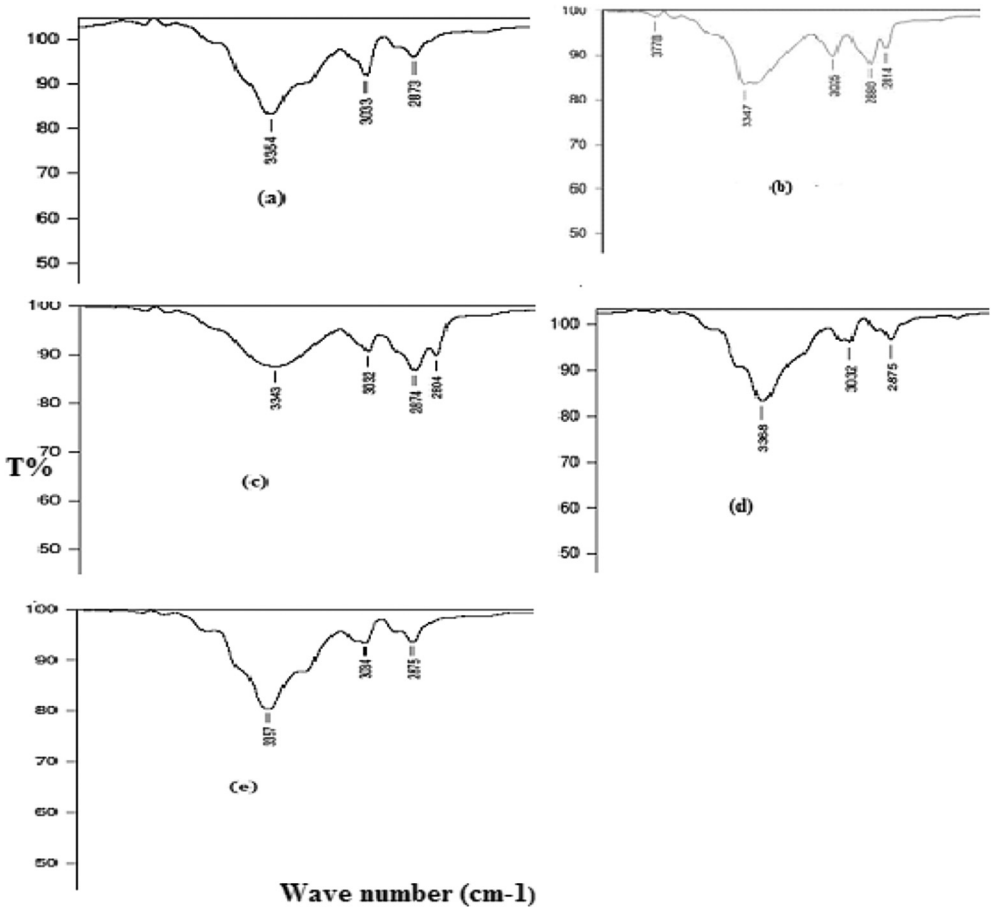

Fig. 4. FT-IR spectra of binary liquid mixtures: benzyl alcohol + aniline (a), benzyl alcohol + N-methylaniline (b), benzyl alcohol + *N,N*-dimethylaniline (c), benzyl alcohol + *o*-chloroaniline (d), benzyl alcohol + *m*-chloro aniline (e).

Table 4
Experimental NMR analysis of the pure and equimolar binary mixture systems at temperature T = 298.15 K.

systems	Band	Experimental	
		Alcohol δ (ppm)	Amine δ (ppm)
benzyl alcohol	OH	3.997	–
Aniline	NH_2 (1^0-amine)	–	3.676
N-methyl aniline	NH (2^0-amine)	–	3.717
N,N-dimethyl aniline	N (3^0-amine)	–	–
o-chloroaniline	NH_2 (1^0-amine)	4.080	–
m-chloroaniline	NH_2 (1^0-amine)	3.737	–
Benzyl alcohol + aniline	OH – NH_2	2.974	3.651
benzylalcohol + N-methyl aniline	OH – NH	2.835	3.690
benzylalcohol + *N,N*-dimethyl aniline	OH – N	3.541	–
benzylalcohol + *o*-chloroaniline	OH – NH_2	3.472	4.098
benzylalcohol + *m*-chloroaniline	OH – NH_2	3.252	3.753

of increased hydrogen bonding strength between binary liquid mixtures. Both OH and NH signals move downfield in H-bonding solvents like CCl_4. According to the data in Table 4, the ^{1}HNMR measurements sensitive to H- Bonding interactions between a liquid mixture of proton (H) and heteroatoms (N, O). But the existence of an H-bond chemical shift values between pure and binary liquid mixtures determined by NMR technique [61]. In the present experimental ^{1}H NMR spectrum study carried out at room temperature. The resultant chemical shift (δ ppm) values of the pure components and equimolar concentration of binary liquid mixtures were given in Table 4 and these spectra are given in Figs. S1 & S2.

The ^{1}H-NMR spectra of five binary liquid mixtures; BA + A (δ 2.974 ppm (-OH), δ 3.651 ppm (-NH_2)), BA + NMA (δ 2.835 ppm (-OH), δ 3.690 ppm (-NH)), BA + N, N-DMA (δ 3.541 ppm (-OH)), BA + *o*-CA (δ 3.472 ppm (-OH), δ 4.098 ppm (-NH_2)), BA + *m*-CA (δ 3.252 ppm (-OH), δ 3.753 ppm (-NH_2)). The magnitude of this difference is entirely dependent on the structure. From Table 4, the chemical shift value of OH protons to move more downfield in the studied binary liquid mixtures fallows the order:

(BA + *o*-CA) > (BA + *m*-CA) > (BA + A) > (BA + NMA).

The weak H- bond formed by the hydrogen on nitrogen of anilines and oxygen atoms of benzyl alcohol molecules has been characterized. But the chemical shift of the binary liquid mixtures depends upon steric hindrance, + I effect of alkyl group present on nitrogen atom. However, it is important to note that the intermolecular hydrogen bond strength depend up on basic character of amines also. Finally, concluded that more downfield shows strong inter molecular hydrogen bond between binary liquid mixtures.

4. Calculations of intermolecular hydrogen bond associations

4.1. Structure and electron density analysis

To investigate the attributes of intermolecular H- bond within the studied liquid mixtures, we can consider fourteen distinct self- and cross-associated complexes have been considered on the nature of the benzyl alcohol and aniline, substituted aniline complexes. The optimized stable structures of complexes **1**–**14** were successfully completed at the B3LYP/6-311++G (d, p) level. The bond structural parameters of complexes **1**–**14** are depicted in Table 5, respectively.

The bond structural parameters of fourteen diverse H- bonding of molecular associations in complexes between benzyl alcohol and aniline, substituted anilines are appeared in Table 5 and Fig. S3. The optimized structures of these dimers are computed at the B3LYP/6-311++G (d, p) level. From this study reveals that various types of H-bond associations are formed between binary mixtures of the donor (X–H) (amine) and acceptor (Y) group of (hydroxyl group) molecules. The analysis of all the ΔR(X–H) (the difference of the X–H bond length associations between monomer complexes) values of hydrogen bonds shows positive. The detailed description of a H-bond parameter, ΔR (H···Y) explained previously [62,63]. From Table 5, the large ΔR (H···Y) value is 0.75596 A^O means that the strong intermolecular O···H–N hydrogen bond in the cross-association of benzyl alcohol and *o*- chloroaniline complex **12**. The intermolecular H-bond strength within the self (pure liquid) and cross-association (mixtures) of all complexes (ΔR (H···Y)) are fallows in the below order:

1(O_2–H_{16}···O_1) > **12**(N_1–H_{14}···O_1) > **14**(N_1–H_{13}···O_1) > **13**(O_1–H_8···N_1) > **8**(O_1–H_8···N_1) > **11**(O_1–H_8···N_1) > **6**(O_1–H_3···N_1) > **5**(N_2–H_{11}···N_1) > **7**(N_1–H_{15}···O_1) > **9**(N_1–H_{13}···O_1) > **10**(O_1–H_8···N_1) > **4**(N_2–H_{11}···N_1) > **3**(N_2–H_{15}···N_1) > **2**(N_1–H_6···N_2).

From, the above analysis the ΔR (H···Y) value indicate that the strength of intermolecular hydrogen bond.

4.2. Natural bond orbital analysis

The interaction energy (ΔE) of the hydrogen bonded complexes and its details given previously [1,64]. According to Table 6, the interaction energies (ΔE^{cp}) absolute for the fourteen hydrogen bond self and cross-associations of the studied binary mixtures given below

12(N_1–H_{14}···O_1) > **14**(N_1–H_{13}···O_1) > **11**(O_1–H_8···N_1) > **13**(O_1–H_8···N_1) > **7**(N_1–H_{15}···O_1) > **9**(N_1–H_{13}···O_1) > **1**(O_2–H_{16}···O_1) > **6**(O_1–H_3···N_1) > **2**(N_1–H_6···N_2) > **4**(N_2–H_{11}···N_1) > **3**(N_2–H_{15}···N_1) > **5**(N_2–H_{11}···N_1) > **8**(O_1–H_8···N_1) > **10**(O_1–H_8···N_1).

The NBO examination has been additionally executed to rely upon the character of ascribed to hydrogen bonds for the fourteen hydrogen bond associations. The stabilization energies, E (2) of all hydrogen bonding binary liquid mixtures were recorded in Table 7. As per Table 7, the NBO investigation displays that the strength order of developing hydrogen bonds in every associations were given below

N_1–H_{14}···O_1 (**12**, 11.23 kJ mol^{-1}) > N_1–H_{13}···O_1 (**14**, 10.11 kJ mol^{-1}) > N_1–H_{15}···O_1 (**7**, 8.83 kJ mol^{-1}) > N_1–H_{13}···O_1 (**9**, 8.43 kJ mol^{-1}) > O_1–H_8···N_1 (**11**, 5.63 kJ mol^{-1}) > O_1–H_8···N_1 (**13**, 5.56 kJ mol^{-1}) > O_1–H_3···N_1 (**6**, 4.73 kJ mol^{-1}) > O_1–H_8···N_1 (**8**,3.47 kJ mol^{-1}) > N_1–H_6···N_2 (**2**, 3.24 kJ mol^{-1}) > N_2–H_{15}···N_1 (**3**,2.95 kJ mol^{-1}) > N_2–H_{11}···N_1(**4**, 2.72 kJ mol^{-1}) > N_2–H_{11}···N_1

Table 6
Interaction energy corrected with BSSE (ΔE. kJ. mol^{-1}) for all dimers at the B3LYP/6-311++G (d, p) level.

Complexes	X-H ….Y	ΔE	BSSE	ΔE^{cp}
1	O_2-H_{16}···O_1	−24.3720	0.73	−23.6420
2	N_1-H_6···N_2	−23.1063	0.72	−22.3863
3	N_2-H_{15}···N_1	−22.8145	0.78	−22.0345
4	N_2-H_{11}···N_1	−23.1472	0.81	−22.3372
5	N_2-H_{11}···N_1	−22.6673	0.78	−21.8873
6	O_1-H_3···N_1	−23.5270	0.79	−22.737
7	N_1-H_{15}···O_1	−29.7513	1.13	−28.6213
8	O_1-H_8···N_1	−22.4273	0.83	−21.5973
9	N_1-H_{13}···O_1	−28.9784	1.19	−27.7884
10	O_1-H_8···N_1	−18. 8091	0.74	−18.0691
11	O_1-H_8···N_1	−28.5732	1.11	27.4632
12	N_1-H_{14}···O_1	−32.2063	0.97	31.2363
13	O_1-H_8···N_1	−23.5478	0.85	22.6978
14	N_1-H_{13}···O_1	−29. 8091	0.77	29.0391

Table 5
Distances (A^0) and angles (^{0}) of the hydrogen bonds for all hydrogen bond associations at the B3LYP/6-311++G (d, p).

Complexes	X-H ….Y	R(X-H)	ΔR (X-H)	R(H …. .Y)	ΔR(H···Y)	R(X … Y)	∠XHY
1	O2-H16···O1	0.97324	0.01150	1.88122	0.83883	2.83927	167.535
2	N1-H6···N2	1.01479	0.00654	2.24327	0.48084	3.22536	168.767
3	N2-H15···N1	1.00947	0.00587	2.26346	0.48654	3.26456	168.443
4	N2-H11···N1	1.01416	0.00611	2.26065	0.48935	3.24571	168.456
5	N2-H11···N1	1.01306	0.00501	2.23963	0.68310	2.9537	157.164
6	O1-H3···N1	0.97490	0.00472	2.02756	0.69244	2.99625	168.968
7	N1-H15···O1	1.01431	0.00769	2.05639	0.66361	2.94961	172.932
8	O1-H8···N1	0.97513	0.00329	2.02736	0.69754	2.81490	176.978
9	N1-H13···O1	1.01319	0.00721	2.13181	0.58819	2.97061	156.687
10	O1-H8···N1	1.01748	0.00361	2.18964	0.58604	3.08223	168.798
11	O1-H8···N1	0.97249	0.00568	2.05246	0.69264	3.03875	163.082
12	N1-H14···O1	1.01382	0.00879	1.99404	0.75596	2.81490	178.110
13	O1-H8···N1	0.97329	0.00476	2.04981	0.70019	3.04165	167.399
14	N1-H13···O1	1.01441	0.00788	2.01894	0.73106	2.82231	174.221

Table 7
Second-perturbation energies (E (2)/kJ · mol^{-1}) of hydrogen bonds for all hydrogen bond associations obtained by NBO analysis at the B3LYP/6-311++G (d, p) level.

Complexes	Donor NBO(i)	Acceptor NBO(j)	E(2)
1	LP(1)O1	BD*(1)O2-H16	1.95
2	LP(1)N2	BD*(1)N1-H6	3.24
3	LP(1)N1	BD*(1)N1-H15	2.95
4	LP(1)N1	BD*(1)N2-H11	2.72
5	LP(1)N1	BD*(1)N2-H11	2.60
6	LP(1)N1	BD*(1)O1-H3	4.73
7	LP(1)O1	BD*(1)N1-H15	8.83
8	LP(1)N1	BD*(1)O1-H8	3.47
9	LP(1)O_1	BD*(1)N1-H13	8.43
10	LP(1)N1	BD*(1)O1-H8	2.33
11	LP(1)N1	BD*(1)O1-H8	5.63
12	LP(1)O_1	BD*(1)N1-H14	11.23
13	LP(1)N1	BD*(1)O1-H8	5.56
14	LP(1)O1	BD*(1)N1-H13	10.11

(**5**,2.60 kJ mol^{-1}) > O_1—H_8···N_1(**10**, 2.33 kJ mol^{-1}) > O_2—H_{16}···O_1 (**1**, 1.95 kJ mol^{-1}).

The above computational results of the second-perturbation energies (E (2)/kJ·mol^{-1}) also predict that the H- bonding cross-associations between benzyl alcohol and 2-chloro aniline(N_1-H_{14}···O_1 bond) is much stronger than the intermolecular cross-associations(O_1-H_8···N_1 bond) of its, because oxygen having more electro negativity than the nitrogen atom and the observed value of V^E from Fig. 1, was negative due to formation of strong inter molecular H-bond associations between the binary liquid mixtures.

From the above computational results said that the intermolecular interaction between benzyl alcohol and aniline, substituted anilines of the binary liquid mixtures were fallows below systematic order:

(BA + *o*-CA) > (BA + *m*-CA) > (BA + A) > (BA + NMA) > (BA + N, N-MA)

Finally, concluded that computational results concur with those of the experimental analysis of FT-IR & ^{1}HN.M.R. Spectroscopy studies.

4.3. Structure and electron density analysis (AIM theory)

Further, perusals of the basic pattern of intermolecular interactions for all five dimers, the reduced density gradient versus sign (λ_2) ρ shown in Fig. 5. According to Yang and co-worker [65,66], one or more low reduced gradient spikes in the low density district indicate interaction of non-covalent bond between liquid mixtures. From, fig (a), fig (b) & fig (c) the negative analysis

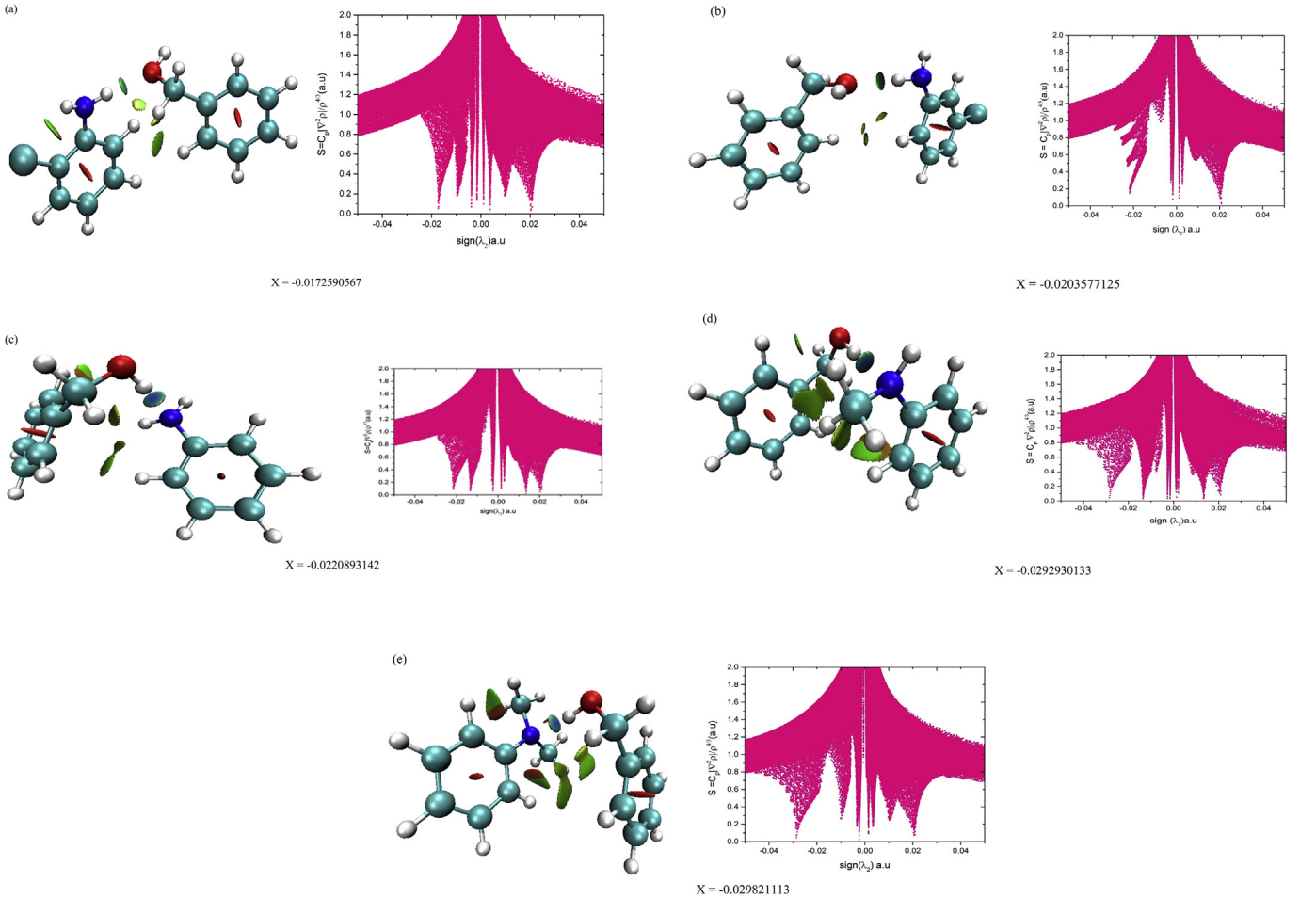

Fig. 5. Plots of the reduced density gradient versus the electron density multiplied by the sign of the second hessian eigenvalues and gradient isosurfaces with s = 0.5 a. u. for the associations of benzyl alcohol with *o*- chloroaniline, *m*- chloroaniline, Aniline, N-methylaniline, *N,N*-dimethyl aniline (fig (a), fig (b), fig (c), fig (d), fig (e)). The surfaces are colored on a blue—green—red scale according to values of sign (λ_2) ρ, ranging from −0.03 to 0.02 a. u. (For interpretation of the references to color in this figure legend, the reader is referred to the Web version of this article.)

values of reduced gradient spike at low density are −0.017,-0.020 and −0.022 a. u. indicates that the stabilizing hydrogen bond interaction between benzyl alcohol and *o*-chloroaniline, *m*-chloroaniline and aniline respectively. Form fig (d) and fig (e), shows more spikes very near zero, denotes weak inter molecular hydrogen bond (−0.0293 to −0.0298 a. u.) between the binary liquid mixtures of benzyl alcohol and *N*- methylaniline and *N, N*-dimethylaniline respectively. So the stabilizing hydrogen bond interaction of all the dimers fallow below order:

BA + *o*-CA (fig (a)) > BA + *m*-CA (fig (b)) > BA + A (fig (c)) > BA + NMA (fig (d)) > BA + N, N-DMA (fig (e))

From Fig. 5, the plots of a blue bonding isosurface has the characteristic sign of strong H- bond between hydrogen donor atom of amino group of substituted aniline and oxygen acceptor of benzyl alcohol and a green bonding isosurface has basic sign of weak inter molecular hydrogen bond between hydrogen donor of -OH group and nitrogen atom of amine acceptor. The general consequence of the gradient isosurface plot examination is totally steady with that of the scatter diagram. Plots of decreased density gradient versus sign $(\lambda_2)\ \rho$ for the all studied systems show one or more spikes in the low density, low-gradient region have an indication of non-covalent interactions. The more negative values of sign $(\lambda_2)\ \rho$ are identification of strong H- bonding interaction. While, the sign $(\lambda_2)\ \rho$ is positive or zero demonstrate very weak H- bonding interactions between binary liquid mixtures.

Finally, an analysis of the gradient isosurfaces, benzyl alcohol with *o*-chloroaniline had more H- bonding interaction than the benzyl alcohol with *m*-chloroaniline, aniline, N-methylaniline, and *N, N*-dimethylaniline. These results had good agreement with the experimental analysis of excess thermodynamic properties, FT-IR and ^{1}H NMR spectroscopy.

4.4. Hydrogen bonding interaction in the liquid phase

Molecular Dynamics (MD) simulations of pure benzylalcohol, aniline, N-methylaniline, *N, N*-dimethylaniline, *o*-chloroaniline and *m*-chloroaniline and mixture of benzyl alcohol with aniline, N-methylaniline, *N,N*-dimethylaniline, *o*-chloroaniline and *m*-chloroaniline was composed of a cubic box containing 200 molecules which were performed using the Gromacs 5.0.4 software package [67]. The structures of components were optimized at the B3LYP/6-31++G** level using Gaussian 03. Further, the details of computational method were discussed earlier [68]. The parameters for bonded and non-bonded interactions were taken from OPLS-AA force field [69].

All simulations were performed in three phases: pre-equilibration, equilibration and production. The pre-equilibration stage involved the construction of the system by placing the particles in a suitable cubic box, performing energy minimization with the Steepest Descend method followed by equilibration in the NVT ensemble. In the equilibration stage, the system was switched to a NPT ensemble and then the system was equilibrated for 1 ns. Finally, the production state was a 10 ns simulation in the NPT ensemble at the specified temperature and a pressure of 1 bar. The Nose−Hoover method was used for the control of pressure and temperature along the simulations. The Ewald summation method [70] with a cutoff radius of 1.2 nm, was applied for Coulombic interaction. All the bonds containing hydrogen atoms were constrained by using LINCS algorithm [71].

For all the systems, initial configurations were generated by randomly placing the appropriate number of molecules of benzylalcohol, aniline and substituted anilines in a cubic simulation box. The radial distribution function (RDF) of pure components was calculated by MD simulations and were given in Fig. S4 (Supplementary). Further, MD simulations can provide information about the H-bonding structures and dynamics on a microscopic level. The structural and dynamic properties of the benzylalcohol with aniline and substituted anilines species are strongly influenced by the hydrogen bonds, particularly by the formation of H-bond between the both species. The intension of using MD, which is a modern theory of liquids is used to calculate the radial distribution function by the statistical thermodynamics [69].

The RDF O···H of pure benzylalcohol given in Fig. S4, HN···N of pure anilines and substituted anilines shown in supplementary Fig. S5. An examination of Fig. S4 suggest that of the two peaks, the first one that is sharp is located at ~1.86 Å^o, and the other one which is wide and weak is located at a distance of ~3.5 Å. The first distance is slightly less than the sum of the van der Waals radii of hydrogen and oxygen atoms [RO···HO ≤ 2.48 Å^o (threshold distance)] [63] which is an indication of intermolecular hydrogen bond between H and O atoms of component molecules. The second distance (3.5 Å^o) which is greater than 2.48 Å^o is not an H-bond. The RDFs of pure aniline and substituted anilines are shown in Fig. S5 for the H_N···N pair. There are two peaks; both of them reveal intermolecular interactions (except N, N-dimethyl aniline). The first peak which appears at 2.2 Å^o is an H-bond (the H_N··· N threshold distance (RN···HN ≤ 2.52 Å)). This H-bond is due to the interaction between N atom of central molecule with the closest HN of other molecules. The second peak (that is greater than 2.52 Å) is located at 3.54 Å^o. This peak also shows intermolecular interactions between N and H atoms.

Fig. 6 shows the intermolecular interaction of N of anilines and HO of benzylalcohol at equimolar ratio and 298.15 K. For the HO···N pair, there are two set of peaks. The first set represents the interaction of N with HO, which is located in the nearest shell, and it can be attributed to H-bonding. Also, due to H-bonding strength, each peak in this set has a specific intensity. The equimolar mixtures of five systems RDF curves have given in Fig. 6 (fig (a), fig (b), fig (c), fig (d), fig (e)). In the present investigation the molecular dynamics simulations in the liquid phase have been constructed RDF curves for the pure and binary liquid mixtures at equimolar. Based on MD simulations, it can be concluded that the H- bonding interaction between HO···HN stronger than the OH···NH between the mixtures of benzylalcohol with aniline and substituted anilines.

5. Summary and conclusions

The main purpose of the present work is to explain the strength of hydrogen bond existence between the binary mixtures of benzylalcohol and aniline, substituted anilines affecting the physical properties of the systems when compared to the individual systems as hydrogen bond involves −OH and $-NH_2$ functional groups. Results on density and speed of sound for benzylalcohol with aniline, substituted anilines at different temperatures have been reported in the present investigation. The data was used to calculate excess molar volumes (V^E) and excess isentropic compressibilities (κ_S^E). The V^E values are negative in all the binary mixtures except the system containing *N,N*-dimethylaniline. The negative data clearly indicating strong attractive interactions between the components-hydrogen bonds and dipole-dipole interactions. The existence of intermolecular hydrogen bonding interactions was additionally confirmed by the FT-IR and ^{1}H-NMR analysis. It can be concluded that thermo physical properties and spectroscopic studies accommodate a comprehensive analysis on the solute- solvent interactions of hydrogen bonding between benzyl alcohol and aniline, substituted anilines. Finally, the above computational results were also coinciding with those of the experimental analysis of excess thermodynamic properties and spectroscopic studies (FT-

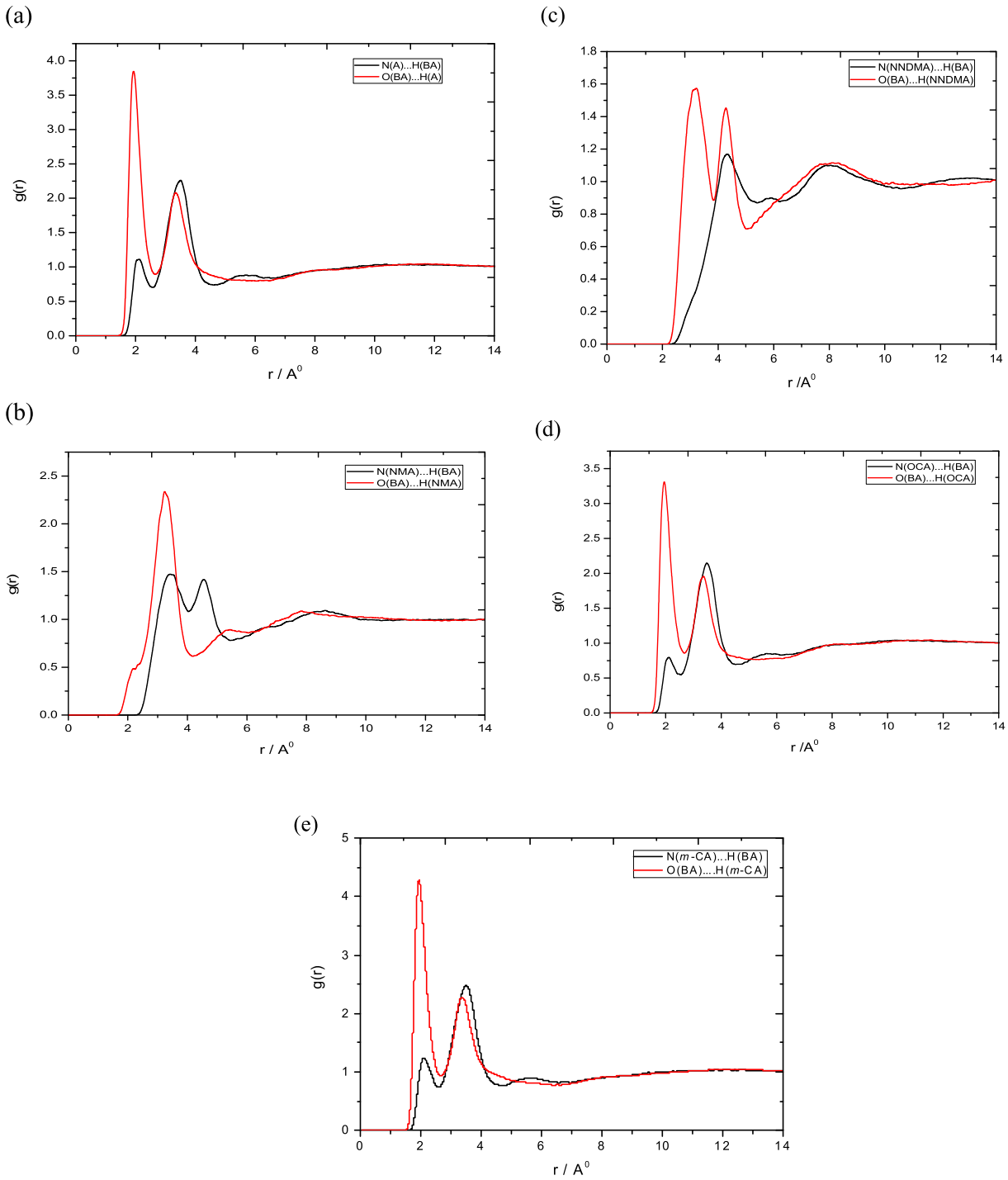

Fig. 6. Radial distribution function for the oxygen of each of the hydroxyl groups of the benzylalcohol and the hydrogen of aniline and substituted anilines. Top and bottom panels show the radial distribution for O···H (red) and N···H (black) in benzylalcohol with aniline (fig (a)), benzylalcohol with N-methylaniline (fig (b)), benzylalcohol with *N,N*-dimethylaniline (fig (c)), benzylalcohol with *o*- chloroaniline (fig (d)), benzylalcohol with *m*-chloroaniline (fig (e)) respectively. (For interpretation of the references to color in this figure legend, the reader is referred to the Web version of this article.)

IR, ^{1}HNMR). The molecular dynamics simulations and DFT calculations supports the existence of H-bonding between benzylalcohol and amines.

Funding

This research did not receive any specific grant from funding agencies in the public, commercial, or not-for-profit sectors.

Acknowledgement

The author M. Raveendra expresses sincere thanks to Prof.P.-Venkateswarlu, Dept. of Chemistry, and Prof. D.V. R. Saigopal, Director DST Purse Centre, S·V.University, Tirupati for providing necessary facilities to carry out ^{1}H NMR Spectral analysis of the present work.

Appendix A. Supplementary data

Supplementary data related to this article can be found at https://doi.org/10.1016/j.fluid.2018.01.025.

References

[1] M. Raveendra, M. Chandrasekhar, C. Narasimharao, L. Venkatramanna, K. Siva Kumar, K. Dayananda Reddy, RSC Adv. 6 (2016) 27335–27348.
[2] V.E. Borisenko, S.A. Krekov, M. YuFomenko, A. Koll, P. Lipkovski, J. Mol. Struct. 882 (2008) 9–23.
[3] R. Dharmendra Singh, L. Gardas, J. Phys. Chem. B 120 (2016) 4834–4842.
[4] A. Cammers-Goodwin, T.J. Allen, S.L. Oslick, K.F. McClure, J.H. Lee, D.S. Kemp, J. Am. Chem. Soc. 118 (1996) 3082–3090.
[5] N. Kimizuka, T. Nakashima, Langmuir 17 (2001) 6759–6761.
[6] J.P. Belieres, D. Gervasio, C.A. Angell, Chem. Commun. 14 (2006) 4799–4801.
[7] B.S. Akpa, C. D'A. gostino, L.F. Gladden, K. Hindle, H. Manyar, J. McGregor, D.W. Rooney, J. Catal. 289 (2012) 30–41.
[8] Kai-Di Chen, Yi-Feng Lin, Chein-Hsiu Tu, J. Chem. Eng. Data 57 (2012) 1118–1127.
[9] R.D. Brimecombe, R. Fogel, J.L. Limson, J. Agric. Food Chem. 54 (2006) 8799–8803.
[10] L. Venkatramana, C. Narasimharao, R.L. Gardas, K. Sivakumar, J. Mol. Liq. 207 (2015) 171–176.
[11] W. Schaaff's, Molekularakustich, Chapter XI and XII, Springer-Verlag, Berlin, 1963. O. Nomoto, J. Phys. Soc. Jpn. 13(1958) 1528–1532.
[12] B. Jacobson, Acta Chem. Scand. 6 (1952) 1485–1498.
[13] B. Jacobson, J. Chem. Phys. 20 (1952) 927–928.
[14] A. Ali, M. Tariq, J. Mol. Liq. 128 (2006) 50–55.
[15] L. Venkatramana, R.L. Gardas, K. Sivakumar, K. Dayananda Reddy, Fluid Phase Equil. 367 (2014) 7–21.
[16] R. Francesconi, A. Bigi, F. Comelli, J. Chem. Eng. Data 50 (2005) 1404–1408.
[17] A. Ali, A.K. Nain, D. Chand, R. Ahmad, Phys. Chem. Liq. 43 (2005) 205–224.
[18] R.L. Gardas, J.A.P. Coutinho, Fluid Phase Equil. 267 (2008) 188–192.
[19] S.J. Kharat, P.S. Nikam, J. Mol. Liq. 131–132 (2007) 81–86.
[20] M.A. Saleh, M. Alauddin, S. Begum, Phys. Chem. Liq. 39 (2001) 453–464.
[21] A.K. Nain, Fluid Phase Equil. 259 (2007) 218–227.
[22] E.B. Freyer, J.C. Hubbard, D.H. Andrews, J. Am. Chem. Soc. 51 (1929) 759–770.
[23] Yan Li, Hong Ye, Pingli Zeng, Feng Qi, J. Solut. Chem. 39 (2010) 219–230.
[24] P.S. Nikam, S.J. Kharat, J. Chem. Eng. Data 48 (2003) 972–976.
[25] R. Palepu, J. Oliver, D. Campbell, J. Chem. Eng. Data 30 (1985) 355–360.
[26] I. Alonso, V. Alonso, I. Mozo, I. Garcıa de la Fuente, J.A. Gonzalez, J.C. Cobos, J. Chem. Eng. Data 55 (2010) 2505–2511.
[27] S.L. Oswal, V. Pandiyan, B. Krishna kumar, P. Vasantharani, Thermochim. Acta 507–508 (2010) 27–34.
[28] V. Pandiyan, P. Vasantharani, S.L. Oswal, A.N. Kannappan, J. Chem. Eng. Data 56 (2011) 269–277.
[29] M. Katz, P.W. Lobo, A.S. Minano, H. Solimo, Can. J. Chem. 49 (1971) 2605–2609.
[30] V. Pandiyan, S.L. Oswal, P. Vasantharani, Thermochim. Acta 518 (2011) 36–46.
[31] B. Nagarjun, A.V. Sarma, G.V. Rama Rao, C. Rambabu, J. Thermoelast. 2013 (2013) 1–9.
[32] G. Manukonda, P. Venkateswarlu, K. Siva kumar, S. Sivarambabu, J. Ind. Eng. Chem. 20 (2013) 405–418. https://doi.org/10.1016/j.jiec.2013.04.035.
[33] M. Anurag, M. Sanjeev, J. Ind. Eng. Chem. 18 (2012) 1013–1017.
[34] Z.R. Master, N.I. Malek, J. Mol. Liq. 196 (2014) 120–134.
[35] V. Pandiyan, S.L. Oswal, N.I. Malek, P. Vasantharani, Thermochim. Acta 524 (2011) 140–150.
[36] P. Jeevanandham, S. Kumar, P. Periyasamy, J. Mol. Liq. 188 (2013) 203–209.
[37] S.S. Joshi, T.M. Aminabhavi, Fluid Phase Equil. 60 (1990) 319–326.
[38] S. kumar, M. Anurag, S. Agarwal, S. Maken, J. Mol. Liq. 155 (2010) 115–120.
[39] J.A. Riddick, W.B. Bunger, T.K. Sakano, Organic Solvents: Physical Properties and Methods of Purification, Wiley Interscience, New York, 1986.
[40] M. Raveendra, C. Narasimharao, L. Venkatramana, K. Sivakumar, K. Dayananda Reddy, J. Chem. Thermodyn. 92 (2016) 97–107.
[41] L. Venkatramana, K. Sivakumar, R.L. Gardas, K. Dayananda Reddy, Thermochim. Acta 581 (2014) 123–132.
[42] M.J. Frisch, G.W. Trucks, H.B. Schlegel, et al., Gaussian 09, Revision D.01, Wallingford, CT, 2009.
[43] S.F. Boys, F. Bernardi, Mol. Phys. 19 (1970) 553.
[44] A.E. Reed, L.A. Curtiss, F. Weinhold, Chem. Rev. 88 (1988) 899–926.
[45] F. Mata, J.M. Leal, B. Garcia, Z. Phys. Chem. (Leipzig) 261 (1980) 1059–1064.
[46] B. García, J.M. Leal, Collect. Czech Chem. Commun. 52 (1987) 299–307.
[47] L.A. Herrero, Tesis Licenciatura, Valladolid Univ., Spain, 1986.
[48] A. Villares, S. Martin, M. Haro, B. Giner, H. Artigas, J. Chem. Therm. 36 (2004) 1027–1036.
[49] G. Douheret, M.I. Davis, J.C.R. Reis, M.J. Blandamer, ChemPhysChem 2 (2001) 148–161.
[50] G.C. Benson, O. Kiyohara, J. Chem. Thermodyn. 11 (1979) 1061–1064.
[51] T.M. Reid, J.M. Prausnitz, B.E. Poling, The Properties of Gases and Liquids, fourth ed., McGraw Hill, New York, 1987.
[52] R. Shaw, J. Chem. Eng. Data 14 (1969) 461–465.
[53] M. Zabransky Jr., V. Ruzicka, J. Phys. Chem. Ref. Data 33 (2005) 1071–1081.
[54] N.I. Malek, S.P. Ijardar, S.B. Oswal, J. Chem. Eng. Data 59 (2014) 540–553.
[55] J.F. Kincaid, H. Eyring, J. Chem. Phys. 6 (1938) 620–629.
[56] P.J. Victor, D.K. Hazra, J. Chem. Eng. Data 47 (2002) 79–82.
[57] O. Redlich, A.T. Kister, Ind. Eng. Chem. 40 (1948) 345–348.
[58] C.A. Hwang, J.C. Holste, K.R. Hall, G.A. Mansoori, Fluid Phase Equil. 62 (1991) 173–189.
[59] R. Dharmendra Singh, L. Gardas, J. Phys. Chem. B 120 (2016) 4834–4842.
[60] R.M. Silverstein, G.C. Bassler, T.C. Morrik, Spectroscopic Identification of Organic Compounds, fifth ed., John Wiley & sons Inc, Singapore, 1991.
[61] Yong-Cheng Ninng, Structural Identification of Organic Compounds with Spectroscopic Techniques, Wiley-VCH, 2005.
[62] C. Guo, H. Fang, R.Y. Huang, H. Xu, G.H. Wu, S.Y. Ye, Chem. Phys. Lett. 588 (2013) 97–101.
[63] A. Bondi, J. Phys. Chem. 68 (1964) 441–451.
[64] S.F. Boys, F. Bernardi, Mol. Phys. 19 (1970) 553–566.
[65] E. D. Gledening, A. E. Reed, J. A. Carpenter, F. Weinhold, NBO. Version. 3.1.
[66] E.R. Johnson, S. Keinan, P. Mori-Sanchez, J. Contreras-Garcia, A.J. Cohen, W. Yang, J. Am. Chem. Soc. 132 (2010) 6498–6506.
[67] D. Van Der Spoel, E. Lindahl, B. Hess, G. Groenhof, A.E. Mark, H.J.C. Berendsen, J. Comput. Chem. 26 (2005) 1701–1718.
[68] S. Ranjbar, A. Soltanabadi, and Z. Fakhri, J. Chem. Eng. Data. DOI:10.1021/acs.jced. 6b00158.
[69] W.L. Jorgensen, D.S. Maxwell, J. Tirado- Rives, J. Am. Chem. Soc. 118 (1996) 11225–11236.
[70] U.L. Essmann, M.L. Perera, T. Berkowitz, H. Darden, H. Lee, L.G. Pedersen, J. Chem. Phys. 103 (1995) 8577–8593.
[71] B. Hess, H. Bekker, H.J.C. Berendsen, J.G.E.M. Fraaije, J. Comput. Chem. 18 (1997) 1463–1472.